

# Interaction of tetanus toxin with lipid vesicles

## Effects of pH, surface charge, and transmembrane potential on the kinetics of channel formation

Gianfranco Menestrina,\* Stefano Forti,\*\* and Franco Gambale<sup>§</sup>

\*Dipartimento di Fisica, Università di Trento, I-38050 Povo, Trento, Italy; <sup>†</sup>Istituto per la Ricerca Scientifica e Tecnologica I-38050 Povo, Trento, Italy; <sup>§</sup>Istituto di Cibernetica e Biofisica, Consiglio Nazionale delle Ricerche and Dipartimento di Fisica, Università di Genova, I-16146 Genova, Italy

**ABSTRACT** We investigated the interaction of tetanus toxin with small unilamellar vesicles composed of different phospholipids as a function of pH, toxin concentration, temperature, and ionic strength of the solution. Tetanus toxin increased the permeability of the vesicles to fluorescent markers of molecular weight up to 700. The time course of the permeabilization was described as the sum of two exponential components of which the faster accounts for more than 70% of the total effect. Both time constants decreased when the pH of the solution was lowered and when vesicles contained negative lipids. These results can be explained in terms of a phenomenological model based on reaction rate theory. The model assumes that tetanus toxin, after

equilibrating with the local pH existing at the surface of the vesicles, inserts into the lipid bilayer forming an ionic channel through which solutes can diffuse. Trigger event for the insertion of the toxin is the protonation, and consequent neutralization of one charged group which makes the molecule more hydrophobic. The intrinsic pK of this group was found to be  $3.4 \pm 0.2$ , suggesting that it may be a carboxyl group. Since the toxin equilibrates with the local pH, the enhancing effect of acidic phospholipids is merely explained by the creation of a negative surface potential which increases the local proton concentration. This was confirmed by the inhibitory effect of high  $\text{Na}^+$  concentration which reduced the surface charge by screening and

specific binding. We found still small differences between the lipids tested and the following order of sensitivity to the action of the toxin: phosphatidylinositol > phosphatidylserine > phosphatidylcholine  $\approx$  cholesterol.

The activation energy for the two time constants was found to be 19.8 and 14.8 kcal/mol, fast and slow component, respectively, i.e., slightly larger than that for pure diffusion through the bilayer.

The permeabilization induced by tetanus toxin is a voltage-dependent process because vesicles bearing an inner negative potential were depolarized very quickly whereas those bearing an inner positive voltage were barely depolarized at all.

## INTRODUCTION

Tetanus toxin (TeTx) is a potent and specific neurotoxin secreted by the bacterium *Clostridium tetanii*. The protein consists of two chains: L (50 kD) and H (100 kD) linked by a disulfide bridge (1–3). It has been proposed that gangliosides GD1b and GT1b or sialoglycoproteins are the membrane receptor for the toxin (4–6). TeTx acts at the level of both the central and the peripheral nervous systems (7). Its paralyzing effects seem to require several steps: binding to nerve terminals, internalization via endocytic vesicles, retrograde axonal transport, and transition to presynaptic neurons (8–10).

It was shown that TeTx increases membrane permeability both in artificial planar bilayers (11–14) and in phospholipid vesicles (15). Interaction of tetanus toxin with membranes is a complex process depending on several parameters such as the pH of the ionic solution, applied transmembrane voltage, and phospholipid compo-

sition of the membrane (11–17). Despite the difference in the target tissues, other bacterial toxins like diphtheria toxin (11, 18), botulinum toxin (11, 19, 20), and exotoxin A from *Pseudomonas aeruginosa* (21) have properties similar to those of tetanus toxin in model systems. The strong dependence of the model membrane–toxin interaction on the pH of the ionic solution, the resistance of mutant cells presenting defective acidification of endosomes (22), and the protective action of amines from attack of toxins (23) have suggested that internalization via endocytic vesicles is a determinant step for the action of these bacterial toxins. The channel-forming properties may be related to this step.

In this study we applied fluorimetric techniques to reveal permeabilization of phospholipid vesicles induced by TeTx with the main purpose of giving a more comprehensive and quantitatively accurate characterization of the chemico-physical parameters controlling the toxin–membrane interaction. Particularly, we investigated (a) the kinetics of the interaction, in order to obtain information on the molecular mechanism of the reactions leading to the formation of the channel; (b) the pH dependence of the toxin insertion using vesicles of different lipid compo-

Correspondence and reprint requests should be addressed to Dr. Menestrina.

sition; and (c) the influence of transmembrane voltage on channel formation in phospholipid vesicles.

These experiments allowed us to present a simple model based on reaction rate theory which may account for our results. The key point of this model is that the insertion of TeTx into a lipid membrane occurs efficiently only when an acidic group of the molecule (pK 3.4) is neutralized by one proton at the surface of the vesicle.

## MATERIALS AND METHODS

### Toxins

TeTx used in this work came from different sources but most of the experiments were performed with a sample made available by Dr. R. Rappuoli of Centro di Ricerche Sclavo, Siena, Italy (hereafter referred to as TeTx.sc). Fragment B of TeTx was purchased from Calbiochem-Behring Corp. (La Jolla, CA) and will be indicated as B-frag.ca. A set of control experiments was run with samples of TeTx and B-fragment kindly provided by Prof. B. Bizzini (Pasteur Institute, Paris) together with a sample of tetanus toxoid, which will hereafter be indicated as TeTx.bb, B-frag.bb, and toxoid.bb. A few control experiments were also carried out with a sample of whole toxin kindly donated by Professor E. Habermann (Liebig Institute, Giessen, FRG). All the proteins were used without further purification. However, before use, samples obtained from Professors B. Bizzini and E. Habermann were extensively dialyzed against the appropriate buffer. SDS gel electrophoresis performed under nonreducing conditions showed that TeTx.bb migrated as two almost indistinguishable 150-kD bands, corresponding to the unreduced toxin, whereas TeTx.sc presented two additional bands of much smaller intensity, at 100 and 50 kD.

Lyophilized  $\delta$ -lysin from *Staphylococcus aureus* (24) was a kind gift of Professor J. Freer (University of Glasgow, UK), and was also used without further purification.

### Preparation of lipid vesicles

Lipids used were egg phosphatidylcholine (PC) from Lipid Products (South Nutfield, UK), phosphatidylserine (PS) and phosphatidylinositol (PI) from Avanti Polar Lipids (Birmingham, AL), and cholesterol from Fluka AG (Buchs, Switzerland). Starting lipid concentration was always 12.5 mg/ml; all binary mixtures were on a 1:1 molar basis. Lipids were always more than 99% pure and gave one single spot by TLC.

Small unilamellar vesicles (SUV) were prepared by sonication, performed (as described in reference 25) in one of the following buffers. Internal buffer A: 70 mM calcein (from Sigma Chemical Co., St. Louis, MO), 50 mM NaCl and enough NaOH to give pH 7.0; internal buffer B: 88 mM 6-carboxy-fluorescein (purchased from Calbiochem-Behring Corp.), 1 mM EDTA, 2 mM TES, and enough NaOH to give pH 7.0. SUV were eluted through a Sephadex G50 column using one of the following buffers. External buffer A: 160 mM NaCl, 2 mM EDTA, 10 mM Hepes, adjusted to pH 7.0 by NaOH; external buffer B: 200 mM NaCl, 2 mM EDTA, 10 mM Hepes adjusted to pH 7.0 by NaOH. Vesicles prepared with internal buffer A and B were washed with external buffer A and B, respectively, in order to remove the untrapped fluorescent marker which was either calcein (710 mol wt), or 6-CF (376 mol wt). All of the external fluorophore was removed by this procedure and SUV (whose average molecular weight is  $\sim 10$  million) eluted in the void volume to a final lipid concentration of  $\sim 2$  mg/mL.

## Marker release experiments

Aliquots of SUV, prepared as described above, were added to a quartz cuvette containing 3 ml of either external buffer A or B and appropriate amounts of KOH and HCl to get the desired pH. The pH was checked to remain constant for the duration of the experiment. In a few experiments the concentration of NaCl in buffer A was varied as specified. The cuvette was continuously stirred and was thermostatted by means of an external circulator to 23°C, if not otherwise specified. Temperature of the cell was tested with a digital thermometer (model 871; Keithley Instruments, Inc., Cleveland, OH). Fluorescence was measured with a model FP550 spectrofluorimeter (Jasco Inc., Easton, MD). For calcein release experiments the excitation wavelength was set at 494 nm (slit width 5 nm) and emission at 520 nm (slit width 10 nm). Calcein release from the interior of the vesicles was detected as an increase of the fluorescence (26). Since the absolute value of fluorescence depends on both the pH of the solution and the concentration of vesicles, 100% of release was determined in each experiment by addition of 0.8 mM Triton X-100. Comparison of the fluorescence produced by 100% of release from fixed amounts of vesicles with a titration curve of pure calcein permitted us to calculate the internal volume of the vesicles. From the surface/volume ratio we estimated their average diameter to be 40–50 nm. This value is in good agreement with reference data (27, 28) and also indicates that the vesicles were actually unilamellar. Spontaneous release of calcein had a half-life of hours under the most unfavorable conditions (SUV composed of pure PC), and could be neglected. 6-Carboxyfluorescein (6-CF) release was similarly detected using excitation at 488 nm and emission at 519 nm (26). Spontaneous release of 6-CF entrapped in PC vesicles could be neglected only when the release induced by TeTx had a time constant shorter than 10 min. No spontaneous release was present when using either PC/cholesterol or PC/PS vesicles.

## Depolarization experiments

To create a transmembrane potential, vesicles composed of egg PC were prepared as described above, either in 200 mM KCl, 5 mM Hepes, 1 mM EDTA, pH 7.0 (buffer C) or in 5 mM KCl, 195 mM TEA-Cl, 5 mM Hepes, 1 mM EDTA, pH 7.0 (buffer D). To get a negative inner potential, vesicles prepared in buffer C were suspended in a cuvette-containing buffer D at the pH indicated in the text, to a final lipid concentration of 50  $\mu$ g/ml. Then valinomycin was added to give a final concentration of 16 nM. For positive inner potentials, vesicles prepared in buffer D were suspended in buffer C and treated as above. Nominal potentials due to the diffusion of K ions can be evaluated from the Nernst equation to be  $\pm 92$  mV, depending on the experimental configuration chosen. Inner potential was measured by adding the hydrophobic anion 8-anilino-naphthalene-1-sulfonate (ANS; 0.6  $\mu$ M). ANS is strongly fluorescent only when bound to lipids (18, 29), and consequently, in the presence of a negative potential, a depolarization results in an increase of the observed fluorescence. On the contrary, however, fluorescence decreased when vesicles bearing a positive inner potential were depolarized. Fluorescence was detected using an excitation wavelength of 380 nm (bandpass 5 nm) and an emission wavelength of 483 nm (bandpass 10 nm), as described above.

## RESULTS

### Permeabilization of lipid vesicles by tetanus toxin

Addition of TeTx.bb to a cuvette containing small unilamellar vesicles loaded with calcein promoted the release

of the dye resulting in an increase of the total fluorescence of the sample (Fig. 1). The time course of the kinetics of interaction could therefore be determined as well as its dependence on several different parameters such as lipid composition of the vesicles, concentration of the toxin, pH, temperature, and ionic strength of the solution. Irrespective of the choice of these parameters, the time course of the interaction could best be fitted by the sum of two exponential components providing two time constants,  $\tau_1$  and  $\tau_2$ , respectively (see inset of Fig. 1). Under most of the experimental conditions, the amplitude of the faster component exceeds that of the slower component by at least a factor of 2–3.

The main features of the interaction of TeTx with SUV did not depend on the kind of fluorescent probe chosen to detect the permeabilizing effects; in fact control experiments performed either with 6-CF (see Fig. 3) or with the complex terbium-dipicolinic acid (30) (data not shown) gave similar results. They did not depend on the preparation of the toxin either, since different samples (i.e., TeTx.sc and TeTx.bb) gave comparable results. However, it must be stressed that samples of fragment B (i.e.,

B-frag.ca and B-frag.bb) gave kinetics of permeabilization which could be fitted by a single time constant.

## pH and surface potential effects on tetanus toxin action

As shown in Fig. 1 the rate of vesicle permeabilization induced by TeTx.bb increased at low pH. For lipid vesicles of different composition and TeTx.sc, the detailed effects of pH on the two time constants  $\tau_1$  and  $\tau_2$  are shown in Fig. 2, A and B, respectively. Results of experiments performed with PC/PS vesicles were intermediate between those of pure PC and pure PS and were omitted for clarity. Pertinent fit parameters were listed in Table 1. With all lipids both time constants increased with the pH. Within one interval they changed approximately by a factor of 10 for each pH unity, suggesting that a direct

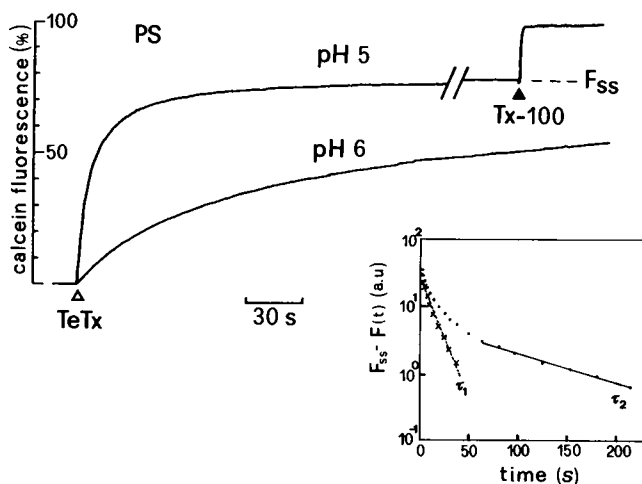


**FIGURE 1** TeTx-induced permeabilization of lipid vesicles loaded with calcein. 278 nM TeTx.bb was added, where indicated by the arrow, to PS vesicles at pH 5 or 6 in external buffer A. Fluorescence,  $F(t)$ , increased after toxin addition, towards a steady state,  $F_{ss}$ , indicating that the dye was released by the vesicles. 100% of release was obtained in each experiment by the addition of 0.8 mM Triton X-100. Final lipid concentration was  $\sim 8 \mu\text{M}$ . (Inset) Half logarithmic plot of the time course of fluorescence change,  $F_{ss} - F(t)$ , at pH 5, measured in arbitrary units. The kinetics can best be fitted by the use of two exponential components. A slow time constant,  $\tau_2$ , can be extrapolated by the last part of the curve, whereas a fast time constant,  $\tau_1$ , is obtained by the first part after subtraction of the slow component. The two time constants found by a least squares method are  $\tau_1 = 12 \text{ s}$  and  $\tau_2 = 100 \text{ s}$ . Correlation coefficient was 0.99 in both cases. The fast and slow time constants for the kinetics at pH 6 were 33 and 275 s, respectively.

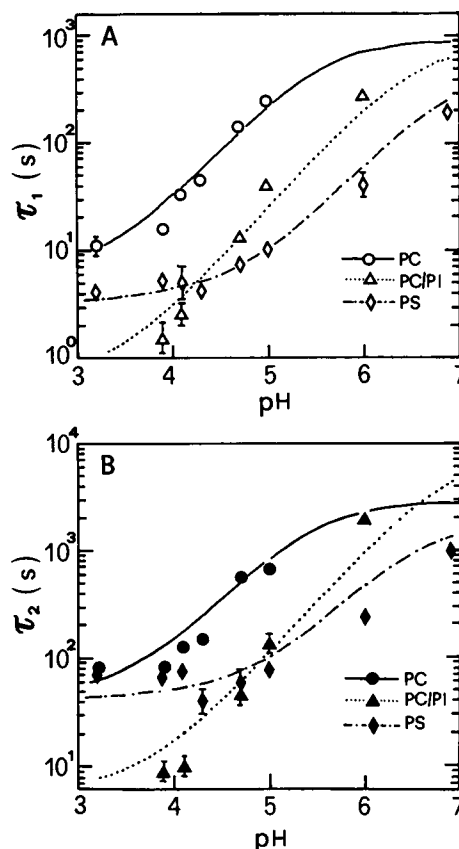


**FIGURE 2** pH dependence of the kinetics of interaction of TeTx with lipid vesicles. TeTx.sc (400 nM) was added to SUV of different composition in external buffer A and the kinetic parameters of calcein release determined as in Fig. 1.  $\tau_1$  and  $\tau_2$  are reported in A and B, respectively, as a function of pH. Different symbols were used for different lipid compositions. Theoretical lines were obtained by the best fit to Eq. 17. The parameters obtained are listed in Table 1. Lipid concentration was as in Fig. 1.

binding of protons to the toxin takes place. Meanwhile, at any fixed pH, both time constants were decreased by using lipid vesicles with increasingly negative surface charge. The results of a parallel set of experiments run with TeTx.bb were similar to those reported in Fig. 2 and were included in Table 1.

In Fig. 3 the effects of pH on TeTx.sc-induced release of 6-CF are reported.

Usually, toxin from a stock solution at pH 6.0 was added to a cuvette containing the vesicles at the desired pH. We also verified that incubation of TeTx.sc at pHs ranging between 2.7 and 3.2 for at least 30 min did not change the time course of permeabilization. This indicates that, even at these extreme values of pH, no irreversible denaturation or self-aggregation of the toxin takes place.

**TABLE 1** Kinetic parameters for the permeabilization of lipid vesicles by tetanus toxin

$\tau_1$							
Agent	Dye	Lipid	pK	$T(A)$	$T(B)$	$k_r(A)$	$k_r(B)$
TeTx.sc	Calc.	PC	3.4	$s$ 900	$s$ 6	$s^{-1}$ 0.133	$s^{-1}$ 20
		PC/PS	3.3	850	5	0.141	24
		PS	3.4	500	3	0.240	40
		PC/PI	2.7	900	0.6	0.133	200
TeTx.bb	Calc.	PC	3.5	600	12	0.288	14.4
		PC/PS	3.4	500	8	0.346	21.6
		PS	4.0	400	8	0.432	21.6
		PC/PI	3.4	400	2	0.432	86.5
TeTx.sc	6-CF	PC or PC/chol	3.4	800	7	0.150	17.1
		PC/PS	3.1	1,000	2	0.120	60

$\tau_2$							
Agent	Dye	Lipid	pK	$T(A)$	$T(B)$	$k_r(A)$	$k_r(B)$
TeTx.sc	Calc.	PC	3.6	$s$ 3,000	$s$ 45	$s^{-1}$ 0.040	$s^{-1}$ 2.7
		PC/PS	3.2	3,000	20	0.040	6
		PS	3.6	2,000	40	0.060	3
		PC/PI	3.0	9,000	6	0.013	20
TeTx.bb	Calc.	PC	3.6	800	45	0.216	3.8
		PC/PS	3.4	800	45	0.216	3.8
		PS	3.6	800	40	0.216	4.3
		PC/PI	3.4	700	12	0.247	14.4
TeTx.sc	6-CF	PC or PC/chol	3.4	4,000	50	0.030	2.4
		PC/PS	3.5	3,500	30	0.034	4

The parameters listed in the table were obtained by the best fit of the experimental data in Figs. 1–2 (and of other data not shown) with Eq. 17. pK is the co-logarithm of the dissociation constant  $K$  of that expression.  $T(A)$  and  $T(B)$  are the asymptotical values of  $\tau$  at high and low pH, respectively, whereas  $k_r(A)$  and  $k_r(B)$  were obtained from  $T(A)$  and  $T(B)$  assuming the validity of Eq. 17 and using the appropriate values for  $v_o$ ,  $\beta$ , and  $T_f$ .

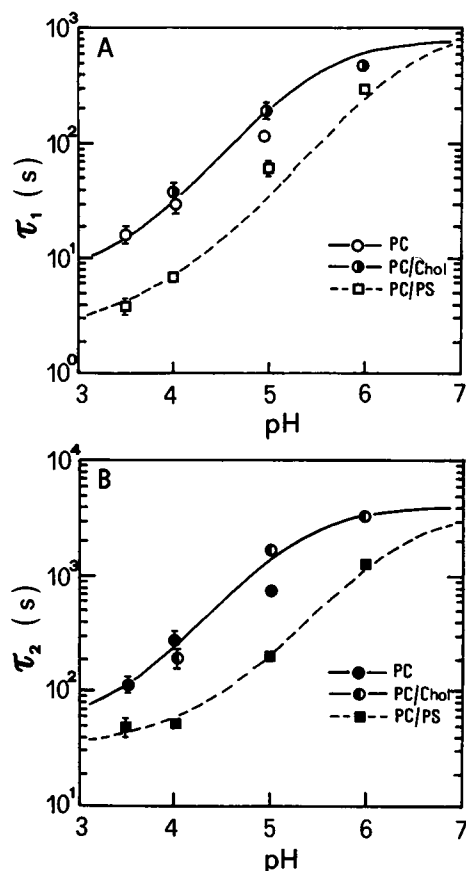


**FIGURE 3** Same as Fig. 2 but using vesicles loaded with 6-CF in external Buffer B. At pH > 5 the spontaneous release of 6-CF from PC vesicles had a halftime comparable to that of toxin-induced release and hence data were not included. PC/cholesterol vesicles did not leak and data could be fitted using the same parameters for PC vesicles, and accordingly only one theoretical line is shown.

## Dependence of the kinetics on toxin and vesicle concentration

As expected for a chemical reaction, both rate constants increased almost linearly with the concentration of the toxin, either in the case of TeTx.sc or in the case of TeTx.bb (Fig. 4, *A* and *B*, respectively). On the other hand, they were almost independent of the vesicle concentration, as illustrated in the case of two different toxin concentrations in Fig. 5 *A*.

A linear increase in the number of permeabilized vesicles (up to a saturation number) was observed when increasing amounts of toxin were sequentially added to the same sample during the same experiment (Fig. 5 *B*). This indicates that there is no cooperativity in the permeabilizing action of TeTx, i.e., that toxin-vesicle interaction is a one-to-one reaction.

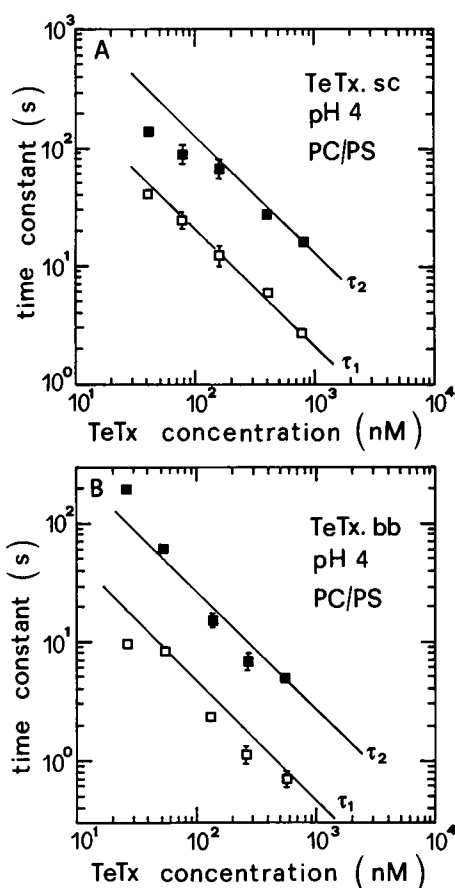


FIGURE 4 Dependence of the kinetics of interaction upon toxin concentration. The two time constants describing the time course of vesicle permeabilization are plotted in a double logarithmic plot against the concentration of TeTx added. TeTx.sc and TeTx.bb were used in *A* and *B*, respectively, on PC/PS vesicles either loaded with 6-CF, in buffer B at pH 4 (*A*), or loaded with calcein in buffer A at pH 4 (*B*). Solid lines were drawn according to Eq. 17, i.e., with a slope of  $-1$ , using the parameters listed in Table 1.

### Dependence of the kinetics on the ionic strength of the solution

Data shown in Figs. 2–3 indicate that TeTx action on lipid vesicles was faster in the presence of negative lipids, possibly because of the reduced local pH in the proximity of the vesicle surface. This interpretation prompted the investigation of the effects of ionic strength on the rate of interaction, since counterions can modulate the surface membrane potential by specific binding as well as by unspecific screening (31).

Consistently, with our hypothesis, it was found that the interaction of TeTx with PC/PS vesicles was progressively slower as the ionic strength of the NaCl solution was increased (Fig. 6).

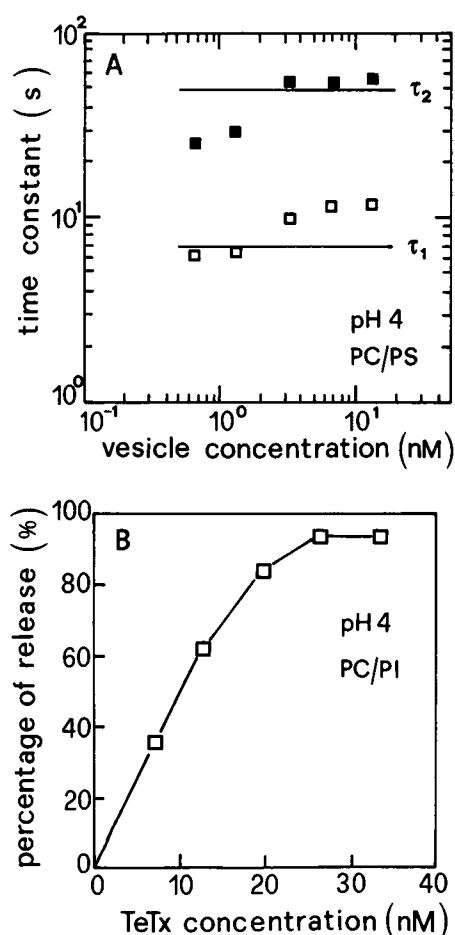


FIGURE 5 Effect of varying the toxin/vesicles ratio on the kinetics of interaction. (*A*) Different amounts of PC/PS vesicles loaded with 6-CF were added to a solution (buffer B) at pH 4 containing 400 nM TeTx.sc. The two time constant of permeabilization are reported in a double logarithmic plot versus vesicle concentration. Solid lines are the predictions of Eq. 17 using the parameters reported in Table 1. (*B*) Increasing amounts of TeTx.sc were added to a cuvette containing PC/PI vesicles, loaded with calcein in buffer A at pH 4. The percentage of lysis was determined as a function of toxin concentration. The linear increase at low toxin concentrations indicates that permeabilization is a one-to-one mechanism.

### Dependence of the kinetics on the temperature

To estimate the activation energy in the reaction between TeTx and lipid vesicles, the temperature dependence of the rate of permeabilization was examined in the range from 5° to 50°C. The results are presented in an Arrhenius plot in Fig. 7 for the case of TeTx.sc and PC/PS vesicles at pH 4. We found a strong coupling between the rate constant and the temperature. There is approximately a fourfold change of  $\tau_1$  and a threefold change of

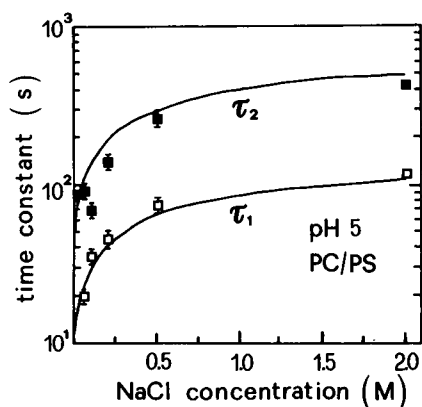


FIGURE 6 Effect of NaCl concentration on the kinetics of toxin-vesicle interaction. 400 nM TeTx.sc were added to a solution containing PC/PS vesicles loaded with calcein (buffer A, pH 5) and different concentrations of NaCl. The two time constants of permeabilization are reported in a half logarithmic plot versus salt concentration. Solid lines are the predictions of Eq. 17 using the parameters reported in Table 1.

$\tau_2$  when raising the temperature from 20°C to the physiological value of 37°C. Similar results were also obtained using PS vesicles at pH 7.0:  $\tau_1$  decreases three times and  $\tau_2$  four times.

Approximately the same temperature dependence was found when TeTx.bb was applied to PS vesicles at pH 7.0:  $\tau_1$  was decreased by a factor of 4 and  $\tau_2$  by a factor of 3.

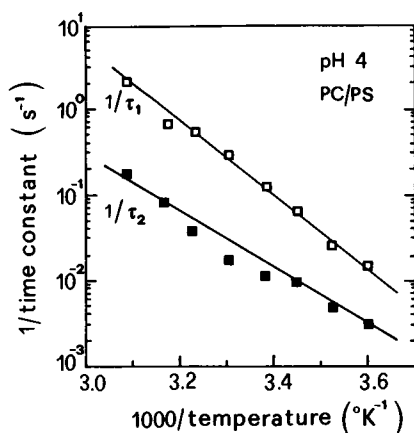


FIGURE 7 Arrhenius plot of the kinetic parameters of toxin-vesicle interaction. 400 nM TeTx.sc were added to a solution containing calcein loaded PC/PS vesicles at different temperatures in Buffer A, pH 4. The reciprocals of the two time constants of permeabilization are reported in a half logarithmic plot versus the reciprocal of the absolute temperature. Solid lines are the predictions of Eq. 17 using the parameters listed in Table 1 and an activation energy of 19.8 kcal/mol for  $\tau_1$  and 14.8 kcal/mol for  $\tau_2$ .

## Dependence of the kinetics on the transmembrane voltage

The results presented so far can easily be understood in terms of the channel-forming properties of TeTx, which were first demonstrated using planar lipid membranes (11, 12). It was shown recently, on that system, that the channel-opening probability strongly increases with the application of a transmembrane voltage, provided that the compartment opposite to that of toxin addition is the negative one (13). This finding prompted us to study the interaction of TeTx with vesicles bearing a 90 mV inner potential either positive or negative (Fig. 8). 100% of depolarization in this case was obtained by addition of another bacterial cytotoxin, i.e.,  $\delta$ -lysin from *Staphylococcus aureus*.

$\delta$ -Lysin, in small concentrations ( $\approx 20 \mu\text{g/ml}$ ), causes complete depolarization of lipid vesicles as well as natural cells (32, 33). We found that vesicles bearing a negative inner potential were strongly depolarized either at pH 4 or at pH 7 by TeTx.sc, and in fact no further depolarization could be obtained by addition of *Staphylococcus aureus*  $\delta$ -lysin (16  $\mu\text{g/ml}$ ). In contrast, vesicles with positive inner potential were barely, if not at all, depolarized by TeTx.sc either at pH 7 or at pH 4 as compared to the action of  $\delta$ -lysin.

The time constants of the depolarization (obtained with the method used in Fig. 1) were less pH dependent in the presence of an internal negative potential. They changed from  $\tau_1 = 13.5 \text{ s}$  and  $\tau_2 = 47.3 \text{ s}$  at pH 7 to  $\tau_1 = 11.6 \text{ s}$  and  $\tau_2 = 25 \text{ s}$  at pH 5. These values can be compared with those in Fig. 2 for the case of unpolarized PC vesicles at pH 5 that are  $\tau_1 = 250$  and  $\tau_2 = 730 \text{ s}$ , i.e., more than 20 times larger. When the internal voltage was positive, even at pH 5, the two time constants were as large as  $\tau_1 = 30$  and  $\tau_2 = 690 \text{ s}$ , not very different from the values for unpolarized vesicles.

## Control experiments

TeTx-induced calcein release from lipid vesicles may, in principle, occur either by formation of a pore large enough to allow the molecule to diffuse through it, or by formation of a narrow pore via a colloid osmotic lysis of the vesicles (24). To discriminate between these two mechanisms we added an osmotic protectant into the external solution. We found that release of calcein was not at all affected by the presence of an isoosmotic concentration of raffinose (600 mol wt) in the external medium (data not shown), indicating that osmotic imbalances are not likely to be involved in the permeabilization process.

We compared the action of TeTx (two different prepa-

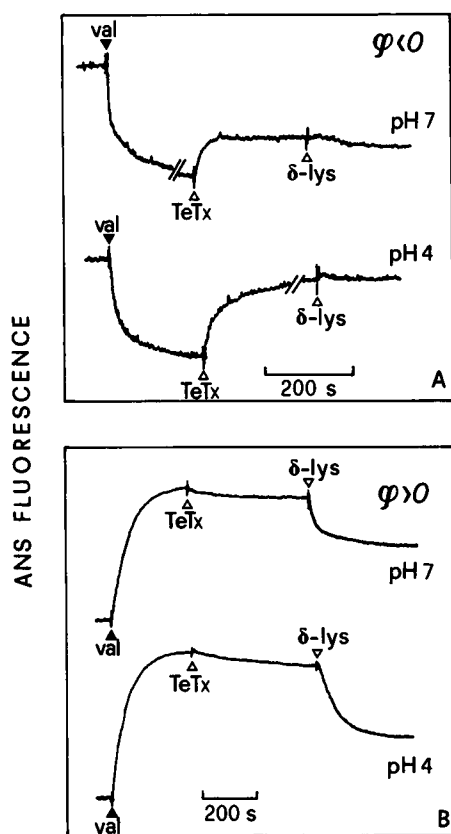


**FIGURE 8** Effects of transmembrane potential on the interaction of TeTx with lipid vesicles. PC vesicles were polarized either at a negative (*A*) or at a positive (*B*) internal voltage by addition of valinomycin in the presence of a transmembrane KCl concentration gradient. Then, 400 nM TeTx.sc were added either at pH 7 (*upper trace* in each panel) or at pH 4 (*lower traces*). With negatively polarized vesicles TeTx caused a strong depolarization at both pH values, and no further depolarization could be obtained by subsequent addition of *Staphylococcus aureus*  $\delta$ -lysin (16  $\mu$ g/ml). Conversely TeTx caused only a weak depolarization of positively polarized vesicles at both pH values, as compared to  $\delta$ -lysin. Membrane potential was estimated by means of the voltage-sensitive fluorescent dye ANS. External buffer C was used in *A* and external buffer D in *B*. Double bars in *A* indicate two interruptions of  $\sim 100$  s (*upper trace*) and  $\sim 200$  s (*lower trace*).

rations), its fragment B, and a derived toxoid, all at the same molar concentration, on PC/PS vesicles. The results, at two different values of pH, are summarized in Table 2. We found that the two toxin preparations behaved similarly, whereas both fragment B and the toxoid were much less active and produced a permeabilization whose time course was described by one single exponential component.

Finally, TeTx.sc tried on planar lipid bilayers induced the formation of fast-fluctuating ionic channels which are voltage and lipid dependent (Gambale, F., unpublished result), and whose characteristics were similar to those

**TABLE 2** Comparison of the effects of tetanus toxin, its fragment B, and a derived toxoid on lipid vesicles

Agent	pH 4.7				pH 3.2			
	$\tau_1$	$\tau_2$	$\tau$	Release	$\tau_1$	$\tau_2$	$\tau$	Release
TeTx.sc	s	s	s	%	s	s	s	%
TeTx.sc	25	160	—	88	6.5	37	—	94
TeTx.bb	34	157	—	75	12	64	—	92
B-frag.bb	—	—	660	12	—	—	275	81
Toxoid.bb	—	—	410	8	—	—	153	66

The kinetic parameters for the permeabilization of lipid vesicles by two preparations of TeTx, by its fragment B, and by a toxoid all at the same molar concentration, 278 nM, are compared at two different values of pH. Time course of permeabilization by TeTx was the sum of two exponential components of time constant  $\tau_1$  and  $\tau_2$  (see Fig. 1), whereas permeabilization by fragment B, and by the toxoid, was well fitted by one single component of time constant  $\tau$ . All the time constants are given in seconds. 100% release was obtained by addition of Triton X-100 as in Fig. 1. Lipid vesicles were comprised of PC/PS and loaded with calcein.

recently described (13, 14) with a different toxin preparation.

## DISCUSSION

We will show in the following that the effects of TeTx on lipid vesicles can be adequately understood within the framework of a model based on reaction rate theory. The model makes a number of assumptions on the mode of action of this toxin. Some of these assumptions will be discussed immediately, others will be introduced later for the sake of clarity.

It is assumed that TeTx interacts with a lipid vesicle, becomes incorporated, and forms a pore permeable to molecules of molecular weight up to 700. This assumption is based on the fact that lipid vesicles are indeed permeabilized by TeTx (Figs. 1 and 8), that the release is neither due to an osmotic swelling (see control experiments), nor to a solubilization of the vesicles of the kind produced by a detergent (because in this case the fluorescence of ANS would never increase, as in Fig. 8 *A*, but always decrease as we checked using Triton X-100), and finally because the formation of ionic channels by TeTx was already postulated in previous papers (11–13, 15, 16, 34).

Because of the small dimensions of our vesicles the formation of just one toxin channel (with a conductance as reported in reference 13), will dissipate the gradient of any permeant molecule within a few milliseconds (35), i.e., much faster than our experimental resolution. This means that the rate-limiting event observed is the formation of channels into the vesicles.

For a description of the channel formation mechanism, we will follow the treatment and the formalism given by Schwarz (36, 37) for the interaction of macromolecules with large aggregates. The insertion of one toxin molecule into the vesicular aggregate is envisaged as a two-step mechanism with the formation of one intermediate "encounter" state,  $T_{enc}$ , populated by toxin molecules which are in close contact with the surface of the vesicles. This state is in equilibrium with free toxin,  $T_f$ , by diffusion in solution, and with inserted toxin,  $T_{ins}$ , by diffusion through the lipid bilayer. Accordingly, the reaction scheme is



where  $k_d$  and  $k_{-d}$  represent the rate of diffusion and back-diffusion of TeTx in the water phase, while  $k_r$  and  $k_{-r}$  represent the same quantities for the lipid phase.

As shown in reference 36, because  $T_{enc}$  is a short-lived state compared to  $T_f$  and  $T_{ins}$  (as it will be demonstrated later), Scheme 1 is actually equivalent to the simpler scheme:



where

$$K_{as} = (k_r k_d) / (k_r + k_{-d}) \quad (3)$$

and

$$K_{dis} = (k_{-r} k_{-d}) / (k_r + k_{-d}). \quad (4)$$

Since the binding of TeTx to lipid vesicles is virtually irreversible (16, 17), it follows that  $k_{-r} = 0$  and also  $K_{dis} = 0$ .

Therefore, from Scheme 2 we have

$$\frac{d[T_{ins}]}{dt} = K_{as} [T_f] [P], \quad (5)$$

where quantities in square brackets are concentrations, and  $[P]$  indicates the total phospholipid available, related to the concentration of vesicles,  $[V]$ , by

$$[P] = [V] \mu \beta. \quad (6)$$

$m$  is the average number of lipid molecules per vesicle, ranging  $1.2\text{--}1.4 \times 10^4$  in our experiments, and  $\beta$  is the fraction of lipid which is located in the outer leaflet,  $\sim 0.62\text{--}0.64$ .

In a typical experiment  $[T_f]$  is 400 nM, while the concentration of vesicles,  $[V]$ , is 0.8 nM. 100% of permeabilization induced by TeTx was not reached in the experiments, implying that some of the vesicles carry no channels at all and hence that only very few vesicles carry

more than one channel. We can thus safely assume that each permeabilized vesicle carries at most one channel, and hence that  $[T_f]$  remains constant throughout the reaction. Accordingly we may write a new rate constant

$$K^* = K_{as} [T_f] \mu \beta. \quad (7)$$

Introducing  $[V]_0$  as the initial concentration of vesicles, we get the following expression for the concentration of unreacted vesicles:

$$[V] = [V]_0 - T_{ins}. \quad (8)$$

Under these conditions Eq. 5 is easily integrated using Eqs. 6–8 to obtain

$$[V] = [V]_0 \exp(-t \cdot K^*). \quad (9)$$

The time constant for the disappearance of intact vesicles is thus

$$\tau = 1/K^*. \quad (10)$$

The total fluorescence,  $F$ , i.e., our observable, is given by  $F_0 ([V]_0 - [V])$ , and changes with time as given by Eq. 9 ( $F_0$  is the average fluorescence increase for the permeabilization of one vesicle).

It is possible to calculate theoretically both  $k_d$  and  $k_{-d}$  since, in the case that no specific interaction develops between toxin and vesicles in the encounter state, they are given by (36)

$$k_d = 4\pi N D R_0 / \mu \quad (11)$$

$$k_{-d} = 4\pi D R_0 / v_o, \quad (12)$$

where  $N$  is Avogadro's number,  $D$  is the coefficient of diffusion of the toxin in solution, and  $R_0$  and  $v_o$  are the radius and volume of the encounter zone, which is assumed to be a spherical shell of radius  $R + L$  around each vesicle, with  $R$  the radius of the vesicle and  $L$  the diameter of the toxin molecule.

Estimates of  $k_d$  and  $k_{-d}$  can be obtained using  $R_0 = 25$  nm (calculated assuming a spherical shape for the toxin in solution and a partial specific volume of  $0.72 \text{ cm}^3/\text{g}$  typical for proteins [38]) and the Stokes-Einstein expression for  $D$ . The resulting values are  $k_d = 6.3 \times 10^5 \text{ M}^{-1} \text{ s}^{-1}$  and  $k_{-d} = 0.33 \times 10^6 \text{ s}^{-1}$ . The average lifetime of the encounter state,  $\tau^*$ , is then

$$\tau^* = 1/k_{-d}, \quad (13)$$

i.e., 3  $\mu\text{s}$ . This lifetime is short enough to justify the assumption that the encounter state is short-lived compared to the other two, but, on the other hand, it is long enough to let the toxin equilibrate with the local pH in the encounter zone as discussed in Appendix A.

Low pH can induce a conformational transition into TeTx promoting the exposition of a hydrophobic region of



the molecule (17, 39). Accordingly, we assume that TeTx at the surface of a vesicle is in a fast, pH-dependent, equilibrium between two different configurations,  $T_{\text{enc}}(\text{A})$  and  $T_{\text{enc}}(\text{B})$ , which have different rates of diffusion into the lipid phase namely  $k_r(\text{A})$  and  $k_r(\text{B})$ . In particular, the diffusion rate of the protonated, "hydrophobic," form,  $k_r(\text{B})$ , is much faster than the other. As demonstrated in Appendix A, because the exchange between the two forms A and B is fast compared to the lifetime of the encounter state, this equilibrium can be taken into account by simply substituting the following for  $k_r$  of Scheme 1:

$$k_r = [k_r(\text{A}) + k_r(\text{B}) H/K] / (1 + H/K), \quad (14)$$

where  $H$  is the proton concentration in the encounter region and  $K$  is the intrinsic dissociation constant for the binding of protons to TeTx.

In the case of vesicles bearing a surface potential,  $\Phi$ , this modulates the local pH through an electrostatic attraction of protons, which can be expressed as

$$H = H_0 \exp(-\Phi/kT), \quad (15)$$

where  $H_0$  is the concentration of protons in the bulk solution. It is possible to evaluate  $H$  for any given set of experimental conditions, such as bulk pH, lipid composition of the vesicles, and ionic strength of the solution, by means of the Gouy-Stern theory (40) as shown in Appendix B.

Combining Eqs. 3, 7, and 10 we get

$$\tau = \left( \frac{k_r k_d}{k_r + k_{-d}} [T_f] \mu\beta \right)^{-1}. \quad (16)$$

$k_r$  has an upper limit in  $k_r(\text{B})$ , that is  $200 \text{ s}^{-1}$  at most in these experiments (see Table 1) and is therefore much smaller than  $k_{-d}$ . With the condition  $k_r \ll k_{-d}$ , and substituting for Eqs. 11 and 12 and 14, we get

$$\tau = \left\{ \frac{k_r(\text{A}) + k_r(\text{B}) (H/K)}{1 + H/K} N v_0 \beta [T_f] \right\}^{-1}, \quad (17)$$

which was used to fit all of the experimental results. According to Eq. 17,  $\tau$  depends on the pH, the charge of the vesicles, and (through the surface potential) the ionic strength of the solution. Furthermore, it is linearly dependent on the reciprocal of toxin concentration, but independent of vesicle concentration. Eventually, through the volume of the encounter zone,  $v_0$ , it is inversely related to the size of the vesicles.

It must be noted that the time course of fluorescence change in our experiments could only be fitted by the sum of two exponential components ( $\tau_1$  and  $\tau_2$ ), suggesting that in this case the mechanism described above might be oversimplified. Alternatively, the two time constants may

result from the microheterogeneity of the entire toxin already mentioned in Materials and Methods. This last possibility is reinforced from the observation that experiments with B-fragment gave a single time constant. For the rest we will assume that the second hypothesis is correct, i.e., the two time constants arise from two simple mechanisms, which function like that outlined above, running in parallel during the experiment. This assumption is also suggested by inspection of Figs. 2–7, which show that both time constants have the same qualitative dependence on all the experimental parameters tried, i.e., pH, lipid composition, toxin and vesicle concentration, temperature, and ionic strength, therefore implying that they represent similar phenomena and not, for example, successive steps of one complex mechanism.

It is worth noting that there are only three free parameters in the expression for  $\tau$ , i.e.,  $k_r(\text{A})$ ,  $k_r(\text{B})$ , and  $K$ . The values of the parameters used to fit the experimental data of Figs. 2–7 are listed in Table 1.  $K$  turns out to be a constant providing an intrinsic pK of  $3.4 \pm 0.2$  for the protonable group of the toxin. This value corresponds to the pH at which TeTx exposes a hydrophobic domain (and irreversibly binds Triton X-100), which is in the range 3.4–3.6 as obtained from Fig. 8 in reference 39. It is also near the intrinsic pK of carboxyl groups on amino acid residues of proteins (41). It is worth stressing that no restrictions have been placed on the value of  $K$  and that experiments shown in Figs. 2–7 were all fitted by the same set of parameters. As for the other assumptions made, the involvement of the surface potential in the activation of the insertion process is proved by the dependence on  $\text{Na}^+$  concentration as shown in Fig. 7, whereas the concentration dependence of Figs. 4 and 5 indicates that TeTx is indeed active as a monomer.

Values of  $k_r(\text{A})$  and  $k_r(\text{B})$  listed in Table 1 have been obtained on the basis of Eq. 17 using appropriate  $v_0$ ,  $\beta$ , and  $[T_f]$ . A discussion of these values should consider that an upper limit to their value is given by unrestricted diffusion of at least part of the protein through the bilayer. The minimum value of this upper limit is given by (36)

$$k_r(\text{diff}) = D^*/Ld, \quad (18)$$

where  $d$  is the thickness of the bilayer and  $D^*$  is the coefficient of diffusion of the protein through the lipid phase. Values of  $D^*$  for proteins can be found in the literature and range  $1\text{--}4 \times 10^{-8} \text{ cm}^2/\text{s}$  (42, 43); accordingly  $k_r(\text{diff})$  ranges  $2\text{--}8 \times 10^4 \text{ s}^{-1}$ .

The largest  $k_r(\text{B})$  we have obtained is  $\sim 2 \times 10^2 \text{ s}^{-1}$ , which is still much smaller than the pure diffusion value, thus indicating the presence of constraints to the motion. Comparison of  $k_r(\text{B})$  obtained with different lipid compositions indicate that the restrictions found increase with the following sequence: PC/PI < PS  $\approx$  PC/PS < PC  $\approx$

PC/cholesterol. One might say that PS, and PI even more, facilitate the insertion of TeTx into the lipid membrane (17, 44) also in analogy to the cases of diphtheria (45) and botulinum toxin (19). However, this specific effect is not very large compared to the effect of the surface charge itself. Extrapolating the theoretical curves obtained with the parameters of Table 1 to the case of zero surface charge, the remaining differences between the time constants with the different lipid compositions are all within a factor of 2.5.

Also the claim that GD1b acts as a receptor for this toxin (4–6, 12, 39) should at least in part be corrected for the contribution of negative surface potential. In fact, the double charge of this molecule (46) alone would give rise to an increase of the rate of interaction (50% in experimental conditions of reference 39).

Values of  $k_r(A)$  depend less on the lipid composition and are always much smaller than the corresponding  $k_r(B)$  (on the average 100 times smaller), indicating that the insertion of the unprotonated form into the vesicle is less favored. One possible explanation for this fact could be that the protonable acidic charge has to become exposed to the hydrophobic interior of the membrane in the inserted form of the toxin, with a consequently high energy cost in form A that is absent in the neutral, protonated form B.

In light of Eq. 17 the activation energy of  $\tau$  is given by the activation energy of  $k_r$ , which, in general, is an average of the activation energies for  $k_r(A)$  and  $k_r(B)$ . However, under the experimental conditions of Fig. 7, the term  $k_r(A)$  is negligible and hence the activation energy can be attributed to the rate constant  $k_r(B)$ . For the purely diffusional case the activation energy of  $k_r(B)$  is expected to coincide with that of  $D^*$ , which is of the order of 12 kcal/mol (42). We found 19.8 kcal/mol for  $\tau_1$  and 14.8 kcal/mol for  $\tau_2$ , indicating the presence of a relatively small extra term.

As far as the transmembrane potential effect is concerned a number of bacterial toxins share a similar voltage dependence, e.g., diphtheria toxin (29, 45), botulinum toxin (11), colicins (47, 48), as well as *Escherichia coli* hemolysin (49). This mechanism, known as voltage-gating, is usually attributed to the movement of electrically charged protein residues through the bilayer. In our case this suggests that one or more positively charged amino acids of tetanus toxin are exposed to the inner compartment of the vesicles when the channel is formed, becoming stabilized there by an internal negative voltage.

At variance with previous results (15, 16, 34) we found that fragment B is much less active than whole toxin on lipid vesicles, as is also the case with the toxoid. At present there is no explanation for this difference, but it may be noticed that the same sequence of potency as measured

here, i.e., TeTx  $\gg$  fragment-B  $\approx$  toxoid has also been found during the binding and the internalization of these proteins into the axons of living animals (50).

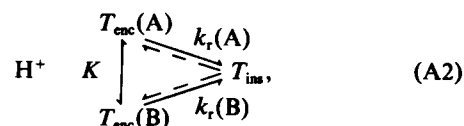
Results shown here were obtained using a relatively high concentration of toxin, in the range of 20–800 nM. Nevertheless the inverse dependence of the time constant of the interaction on the size of the target (which is inherent into Eq. 17) implies a much faster action of this toxin on natural cells, whose radius is  $10^2$ – $10^3$  times larger than that of our vesicles. It follows that living cells might in principle be affected fast enough even at toxin concentrations 4 to 6 orders of magnitude smaller than those used here.

## APPENDIX A

In this section the scheme



is developed into scheme



in which it is assumed that toxin molecules in the encounter state can bind or lose protons very quickly, fluctuating between a protonated (B) and an unprotonated (A) form. Both of these forms can, in principle, diffuse into the lipid bilayer to produce the same final inserted species, but with largely different rate constants. Forward rate constants are  $k_r(A)$  and  $k_r(B)$ , from state A and B, respectively, whereas backward rate constants are assumed to be very small, virtually nil.

Accordingly we may write

$$\frac{d[T_{\text{ins}}]}{dt} = k_r(A) [T_{\text{enc}}(A)] + k_r(B) [T_{\text{enc}}(B)]. \quad (\text{A3})$$

The protonation reaction is assumed to be so fast that it is always at equilibrium during the lifetime of  $T_{\text{enc}}$ , and therefore we have

$$[T_{\text{enc}}(B)] = [T_{\text{enc}}(A)] (H/K), \quad (\text{A4})$$

where  $H$  is the local concentration of protons and  $K$  is the dissociation constant of the protonation reaction.

From the law of conservation of mass we also get

$$[T_{\text{ins}}] + [T_{\text{enc}}(A)] + [T_{\text{enc}}(B)] = T_0, \quad (\text{A5})$$

where  $T_0$  is a constant.

Substituting for Eqs. A4 and A5 into Eq. A3 one gets

$$\frac{d[T_{\text{enc}}(A)]}{dt} = - \frac{k_r(A) + (H/K) k_r(B)}{1 + H/K} [T_{\text{enc}}(A)], \quad (\text{A6})$$

which is easily integrated to give

$$[T_{\text{enc}}(A)] = [T_{\text{enc}}(A)]_0 \exp(-k^* t), \quad (\text{A7})$$

where  $[T_{\text{enc}}(A)]_0$  is the initial value of  $[T_{\text{enc}}(A)]$  and  $k^*$  is

$$k^* = \frac{k_r(A) + (H/K) k_r(B)}{1 + H/K}. \quad (\text{A8})$$

Assuming the initial condition  $[T_{\text{int}}]_0 = 0$ , we finally get

$$[T_{\text{int}}] = T_0 [1 - \exp(-k^* t)]. \quad (\text{A9})$$

Eq. A9 is actually equivalent to what one would have obtained from the simpler scheme A1 (for the case that  $k_{-r}$  is nil) provided that

$$k_r = k^*, \quad (\text{A10})$$

which is the expression used in the text.

That the lifetime of the encounter state is long compared to those of the two configurations A and B is warranted by the exceedingly high rate of diffusion of protons in water solutions. Data in the literature report that the rate of protonation,  $K_p$ , of a macromolecule adsorbed on the surface of a micelle is in the range  $5\text{--}10 \times 10^{10} \text{ M}^{-1}\text{s}^{-1}$  (51, 52), and a value even higher,  $4 \times 10^{11} \text{ M}^{-1}\text{s}^{-1}$ , was found for the protonation of a  $\text{Ca}^{++}$  channel in natural cells (53). The rate of deprotonation,  $K_d$ , can be calculated in our case from the pK of the reaction (which is 3.4 as taken from Table 1) in  $3 \times 10^7 \text{ s}^{-1}$ , using  $K_p = 10 \times 10^{10} \text{ M}^{-1}\text{s}^{-1}$ . An upper limit to the time necessary to reach equilibrium can be taken as  $3\tau_H$  where

$$\tau_H = 1/(K_p H + K_d). \quad (\text{A11})$$

$3\tau_H$  ranges 3–90 ns in our case, i.e., actually much less than the average lifetime of the encounter state, which is 3  $\mu\text{s}$ .

## APPENDIX B

The local pH at the surface of a phospholipid vesicle containing acidic lipids can be calculated according to the Gouy-Stern theory (31, 40, 46).

If we call  $\Phi$  the surface potential, the following set of equations holds:

$$\sin h(e\Phi/2kT) = A\sigma\sqrt{Na_0} \quad (\text{B1})$$

$$\sigma = \sigma_{\text{max}}/(1 + H/K_H + Na/K_{Na}) \quad (\text{B2})$$

$$H = H_0 \exp(-\Phi/kT) \quad (\text{B3})$$

$$Na = Na_0 \exp(-\Phi/kT), \quad (\text{B4})$$

where  $H$  and  $H_0$  are the concentration of protons at the surface of the vesicles and in the bulk solution, respectively.  $Na$  and  $Na_0$  are the surface and bulk concentration of  $\text{Na}^+$  ions,  $\sigma$  and  $\sigma_{\text{max}}$  the actual and the maximal charge density on the surface of the vesicles,  $K_H$ ,  $K_{Na}$  the dissociation constants for the binding of  $\text{H}^+$  and  $\text{Na}^+$  to phospholipids.  $N$ ,  $e$ ,  $k$ , and  $T$  have their usual meaning and  $A$  is given by

$$A = 1/\sqrt{(8N\epsilon_0 kT)}, \quad (\text{B6})$$

where  $\epsilon_0$  is the dielectric constant of water.

Values of  $K_H$  and  $K_{Na}$  are given in the literature; for the case of PS in lipid vesicles one gets  $K_H = 5 \times 10^{-4} \text{ M}$  (54–56) and  $K_{Na} = 1.67 \text{ M}$  (31); for PI instead  $K_H$  is larger than 0.1 M because only the phosphate group is present as a possible substrate (57) and the binding of cations is negligible (58). Similarly, PC does not appreciably bind either protons or monovalent cations at these concentrations (31).  $\sigma_{\text{max}}$  has been

calculated as one electron charge every 70  $\text{\AA}^2$  for the case of PS vesicles, or 0.24 C/m<sup>2</sup>. For PC/PS or PC/PI vesicles one has to take into account the tendency for these lipids to concentrate on the inner leaflet of unilamellar vesicles (59). From published data on sonicated vesicles we could estimate a ratio PS(int)/PS(ext) = 3:1 in our preparation and the same for PI (60, 61); this reduces  $\sigma_{\text{max}}$  to less than half that of PS vesicles, i.e., to 0.06–0.07 C/m<sup>2</sup>.

Solving Eqs. B1–B4 numerically we determined the value of  $H$  as a function of  $H_0$ ,  $Na_0$ , and  $\sigma_{\text{max}}$  for the different lipid compositions used, which we then introduced into Eq. 17.

We thank B. Bizzini, J. Freer, E. Habermann, and R. Rappuoli for kindly donating most of the protein samples used, S. Oiki for helpful discussions, M. Montal and N. Duzgunes for their comments on the manuscript, and C. Pederzoli for performing SDS gel electrophoresis. C. Presti kindly checked the English.

The authors were financially supported by the Italian Consiglio Nazionale delle Ricerche and Ministero di Pubblica Istruzione.

Received for publication 9 June 1988 and in final form 22 September 1988.

## REFERENCES

1. Matsuda, M., and M. Yoneda. 1975. Isolation and purification of two antigenically active, "complementary" polypeptide fragments of tetanus neurotoxin. *Infect. Immun.* 12:1147–1153.
2. Helting, T. B., and O. Zwisler. 1977. Structure of tetanus toxin. I. Breakdown of the toxin molecule and discrimination between polypeptide fragments. *J. Biol. Chem.* 252:187–193.
3. Eisel, U., W. Jarausch, K. Goretzki, A. Henschen, J. Engels, U. Weller, M. Hudel, E. Habermann, and H. Niemann. 1986. Tetanus toxin: primary structure, expression in *E. coli*, and homology with botulinum toxins. *EMBO (Eur. Mol. Biol. Organ.) J.* 5:2495–2502.
4. Bizzini, B., P. Grob, and K. Akert. 1981. Papain-derived fragment II<sub>c</sub> of tetanus toxin: its binding to isolated synaptic membranes and retrograde axonal transport. *Brain Res.* 210:291–299.
5. Fishman, P. H. 1982. Role of membrane gangliosides in the binding and action of bacterial toxins. *J. Membr. Biol.* 69:85–97.
6. Critchley, D. R., W. H. Habig, and P. H. Fishman. 1986. Reevaluation of the role of gangliosides as receptors for tetanus toxin. *J. Neurochem.* 47:213–222.
7. Bizzini, B. 1979. Tetanus toxin. *Microbiol. Rev.* 43:224–240.
8. Simpson, L. L. 1986. Molecular pharmacology of botulinum toxin and tetanus toxin. *Annu. Rev. Pharmacol. Toxicol.* 26:427–453.
9. Mellanby, J., and J. Green. 1981. How does tetanus toxin act? *Neurosci.* 6:281–300.
10. Bizzini, B. 1976. Tetanus toxin structure as a basis for elucidating its immunological and neuropharmacological activities. *In Receptors and Recognition, Series B. The Specificity and Action of Animal, Bacterial and Plant Toxins.* P. Cuatrecasas, ed. Chapman and Hall, UK. 176–217.
11. Hoch, D. H., M. Romero-Mira, B. E. Ehrlich, A. Finkelstein, B. R. DasGupta, and L. L. Simpson. 1985. Channels formed by botulinum, tetanus, and diphtheria toxins in planar lipid bilayers: relevance to translocation of proteins across membranes. *Proc. Natl. Acad. Sci. USA.* 82:1692–1696.

12. Borochoy-Neori, H., E. Yavin, and M. Montal. 1984. Tetanus toxin forms channels in planar lipid bilayers containing gangliosides. *Biophys. J.* 45:83–85.
13. Gambale, F., and M. Montal. 1988. Characterization of the channel properties of tetanus toxin in planar lipid bilayers. *Biophys. J.* 53:771–783.
14. Gambale, F., and M. Montal. 1987. Tetanus toxin forms transmembrane channels in lipid bilayers at neutral pH. *Soc. Neurosci. Abstr.* 13:96.
15. Boquet, P., and E. Duflo. 1982. Tetanus toxin fragment forms channels in lipid vesicles at low pH. *Proc. Natl. Acad. Sci. USA.* 79:7614–7618.
16. Roa, M., and P. Boquet. 1985. Interaction of tetanus toxin with lipid vesicles at low pH. *J. Biol. Chem.* 260:6827–6835.
17. Montecucco, C., G. Schiavo, J. Brunner, E. Duflo, P. Boquet, and M. Roa. 1986. Tetanus toxin is labeled with photoactivatable phospholipids at low pH. *Biochemistry.* 25:919–924.
18. Shiver, J. W., and J. J. Donovan. 1987. Interactions of diphtheria toxin with lipid vesicles: determinants of ion channel formation. *Biochim. Biophys. Acta.* 903:48–55.
19. Shone, C. C., P. Hambleton, and J. Melling. 1987. A 50-kDa fragment from the NH<sub>2</sub>-terminus of the heavy subunit of *Clostridium botulinum* type A neurotoxin forms channels in lipid vesicles. *Eur. J. Biochem.* 167:175–180.
20. Donovan, J. J., and J. L. Middlebrook. 1986. Ion-conducting channels produced by botulinum toxin in planar lipid membranes. *Biochemistry.* 25:2872–2876.
21. Zalman, L. S., and B. J. Wiesnisky. 1985. Characterization of the insertion of *Pseudomonas* exotoxin A into membranes. *Infect. Immun.* 50:630–635.
22. Merion, M., P. Schlesinger, R. M. Brooks, J. M. Moehring, T. J. Moehring, and W. S. Sly. 1983. Defective acidification of endosomes in chinese hamster ovary cell mutants "cross-resistant" to toxins and viruses. *Proc. Natl. Acad. Sci. USA.* 80:5315–5319.
23. Leppla, S. H., R. B. Dorland, and J. L. Middlebrook. 1980. Inhibition of diphtheria toxin degradation and cytotoxic action by chloroquine. *J. Biol. Chem.* 255:2247–2250.
24. Freer, J. H. 1982. Cytolytic toxins and surface activity. *Toxicon.* 20:217–221.
25. Menestrina, G. 1988. *Escherichia coli* hemolysin permeabilizes small unilamellar vesicles by a single hit mechanism. *FEBS (Fed. Eur. Biochem. Soc.) Lett.* 232:217–220.
26. Kayalar, C., and N. Duzgunes. 1986. Membrane action of Colicin E1: detection by the release of carboxyfluorescein and calcein from liposomes. *Biochim. Biophys. Acta.* 860:51–56.
27. Hammond, K., M. D. Reboiras, I. G. Lyle, and M. N. Jones. 1984. Characterization of phosphatidylcholine/phosphatidylinositol sonicated vesicles. Effects of phospholipid composition on vesicle size. *Biochim. Biophys. Acta.* 774:19–25.
28. Reers, M., R. Elbracht, H. Rudel, and F. Spenner. 1984. Rapid methods for the characterization of unilamellar phospholipid vesicles. Application to study of fatty acid donor and acceptor properties of membranes and fatty acid binding proteins. *Chem. Phys. Lipids.* 36:15–28.
29. Slavik, J. 1982. Anilinoaphthalene sulfonate as a probe of membrane composition and function. *Biochim. Biophys. Acta.* 694:1–25.
30. Belmonte, G., L. Cescatti, B. Ferrari, T. Nicolussi, M. Ropele, and G. Menestrina. 1987. Pore formation by *Staphylococcus aureus* alpha-toxin in lipid bilayers: dependence upon temperature and toxin concentration. *Eur. Biophys. J.* 14:349–358.
31. Eisenberg, M., T. Gresalfi, T. Riccio, and S. McLaughlin. 1979. Adsorption of monovalent cations to bilayer membranes containing negative phospholipids. *Biochemistry.* 18:5213–5223.
32. Bhakoo, M., T. H. Birkbek, and J. Freer. 1985. Phospholipid-dependent changes in membrane permeability induced by staphylococcal  $\delta$ -lysin and bee venom melittin. *Can. J. Biochem. Cell Biol.* 63:1–6.
33. Yianni, Y. P., J. E. Fitton, and C. G. Morgan. 1986. Lytic effects of melittin and  $\delta$ -haemolysin from *Staphylococcus aureus* on vesicles of dipalmitoylphosphatidylcholine. *Biochim. Biophys. Acta.* 856:91–100.
34. Boquet, P., and E. Duflo. 1984. Fragment B of tetanus toxin forms channels in lipid vesicles at low pH. In *Bacterial Protein Toxins.* J. E. Alouf, F. J. Fehrenbach, J. H. Freer, and J. Jeljaszewicz, editors. Academic Press, London. 421–426.
35. Miller, C. 1984. Ion channels in liposomes. *Annu. Rev. Physiol.* 46:549–558.
36. Schwarz, G. 1987. Basic kinetics of binding and incorporation with supramolecular aggregates. *Biophys. Chem.* 26:163–169.
37. Schwarz, G., H. Gerke, V. Rizzo, and S. Stankowsky. 1987. Incorporation kinetics in a membrane, studied with the pore-forming peptide alamethicin. *Biophys. J.* 52:685–692.
38. Bhakdi, S., and J. Tranum-Jensen. 1981. Molecular weight of the membrane C5b-9 complex of human complement: characterization of the terminal complex as a C5b-9 monomer. *Proc. Natl. Acad. Sci. USA.* 78:1818–1822.
39. Boquet, P., E. Duflo, and B. Houttecoeur. 1984. Low pH induces a hydrophobic domain in the tetanus toxin molecule. *Eur. J. Biochem.* 144:339–344.
40. Aveyard, R., and D. A. Haydon. 1973. *An Introduction to the Principles of Surface Chemistry.* University Press, Cambridge.
41. Martell, A. E., and R. M. Smith. 1977. *Critical Stability Constants.* Plenum Publishing Corp., New York.
42. Vaz, W. L. C., M. Criado, V. M. C. Madeira, G. Schoellman, and T. M. Jovin. 1982. Size dependence of the translational diffusion of large integral membrane proteins in liquid-crystalline phase lipid bilayers. A study using fluorescence recovery after photobleaching. *Biochemistry.* 21:5608–5612.
43. Vaz, W. L. C., F. Goodsaid-Zalduondo, and K. Jacobson. 1984. Lateral diffusion of lipids and proteins in lipid bilayer membranes. *FEBS (Fed. Eur. Biochem. Soc.) Lett.* 174:199–207.
44. Cabiaux, V., P. Lorge, M. Vandenbranden, P. Falmagne, and J. M. Ruyschaert. 1985. Tetanus toxin induces fusion and aggregation of lipid vesicles containing phosphatidylinositol at low pH. *Biochem. Biophys. Res. Commun.* 128:840–849.
45. Donovan, J. J., M. I. Simon, and M. Montal. 1982. Insertion of diphtheria toxin into and across membranes: role of phosphoinositide asymmetry. *Nature (Lond.).* 298:669–672.
46. McDaniel, R. V., A. McLaughlin, A. P. Winiski, M. Eisenberg, and S. McLaughlin. 1984. Bilayer membranes containing the ganglioside G<sub>M1</sub>: models for electrostatic potentials adjacent to biological membranes. *Biochemistry.* 23:4618–4624.
47. Schein, S. J., B. L. Kagan, and A. Finkelstein. 1978. Colicin K acts by forming voltage-dependent channels in phospholipid bilayer membranes. *Nature (Lond.).* 276:159–163.
48. Davidson, V. L., K. R. Brunden, W. A. Cramer, and F. S. Cohen. 1984. Studies on the mechanism of action of channel-forming colicins using artificial membranes. *J. Membr. Biol.* 79:105–118.

49. Menestrina, G., N. Mackman, I. B. Holland, and S. Bhakdi. 1987. *Escherichia coli* haemolysin forms voltage-dependent channels in lipid membranes. *Biochim. Biophys. Acta.* 905:109–117.
50. Weller, U., C. F. Taylor, and E. Habermann. 1986. Quantitative comparison between tetanus toxin, some fragments and toxoid for binding and axonal transport in the rat. *Toxicon.* 24:1055–1063.
51. Gutman, M., E. Nachliel, E. Gershon, and R. Giniger. 1983. Kinetic analysis of the protonation of a surface group of a macromolecule. *Eur. J. Biochem.* 134:63–69.
52. Gutman, M., and E. Nachliel. 1985. Kinetics analysis of protonation of a specific site on a buffered surface of a macromolecular body. *Biochemistry.* 24:2941–2946.
53. Prod'homme, B., D. Pietrobon, and P. Hess. 1987. Direct measurement of proton transfer rates to a group controlling the dihydropyridine-sensitive  $\text{Ca}^{2+}$  channel. *Nature (Lond.).* 329:243–246.
54. Tsui, F. C., D. M. Ojcius, and W. L. Hubbel. 1986. The intrinsic  $\text{pK}_a$  values for phosphatidylserine and phosphatidylethanolamine in phosphatidylcholine host bilayers. *Biophys. J.* 49:459–468.
55. Cevc, G., A. Watts, and D. Marsh. 1981. Titration of the phase transition of bilayer membranes. Effects of pH, surface electrostatics, ion-binding, and head-group hydration. *Biochemistry.* 20:4955–4965.
56. MacDonald, R. C., S. A. Simon, and E. Baer. 1976. Ionic influences on the phase transition of phosphatidylserine. *Biochemistry.* 15:885–891.
57. Sundler, R., N. Duzgunes, and D. Papahadjopoulos. 1981. Control of membrane fusion by phospholipid head groups. II. The role of phosphatidylethanolamine in mixtures with phosphatidate and phosphatidylinositol. *Biochim. Biophys. Acta.* 649:751–758.
58. Sundler, R., and D. Papahadjopoulos. 1981. Control of membrane fusion by phospholipid head groups. I. Phosphatidate/phosphatidylinositol specificity. *Biochim. Biophys. Acta.* 649:743–750.
59. Op den Kamp, J. A. F. 1979. Lipid Assymetry in Membranes. *Annu. Rev. Biochem.* 48:47–71.
60. Berden, J. A., R. W. Barker, and G. K. Radda. 1975. NMR studies on phospholipid bilayers. Factors affecting lipid distribution. *Biochim. Biophys. Acta.* 375:186–208.
61. Barker, R. W., K. Barret-Bee, J. A. Berden, C. E. McCall, and G. K. Radda. 1975. Sidedness and location of small molecules in membranes. *Chem. Abstr.* 83:173.